This article was downloaded by: [Renmin University of China]
On: 13 October 2013, At: 11:08
Publisher: Taylor & Francis
Informa Ltd Registered in England and Wales Registered Number: 1072954 Registered office: Mortimer House, 37-41 Mortimer Street, London W1T 3JH, UK

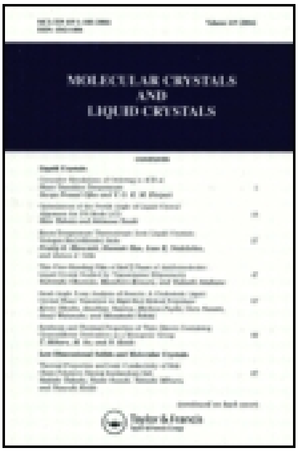

Molecular Crystals and Liquid Crystals
Publication details, including instructions for authors and subscription information:
http://www.tandfonline.com/loi/gmcl20

Surface Engineering of Zinc Oxide Nanoparticles by Biocompatible PPEGMA Polymer: Synthesis, Characterization, and Optical Property Studies

Md. Rafiqul Islam [a], Long Giang Bach [a], Sang-Jin Jung [b], Yeong-Soon Gal [c] & Kwon Taek Lim [a]

[a] Department of Imaging System Engineering, Pukyong National University, Busan, Korea

[b] Department of Advanced Materials Engineering, Kyungsung University, Busan, Korea

[c] College of General Education, Kyungil University, Kyungsangbuk-Do, Hayang, Korea

Published online: 11 Sep 2013.

To cite this article: Md. Rafiqul Islam, Long Giang Bach, Sang-Jin Jung, Yeong-Soon Gal & Kwon Taek Lim (2013) Surface Engineering of Zinc Oxide Nanoparticles by Biocompatible PPEGMA Polymer: Synthesis, Characterization, and Optical Property Studies, Molecular Crystals and Liquid Crystals, 580:1, 39-46, DOI: 10.1080/15421406.2013.803912

To link to this article: http://dx.doi.org/10.1080/15421406.2013.803912

PLEASE SCROLL DOWN FOR ARTICLE

Taylor & Francis makes every effort to ensure the accuracy of all the information (the "Content") contained in the publications on our platform. However, Taylor & Francis, our agents, and our licensors make no representations or warranties whatsoever as to the accuracy, completeness, or suitability for any purpose of the Content. Any opinions and views expressed in this publication are the opinions and views of the authors, and are not the views of or endorsed by Taylor & Francis. The accuracy of the Content should not be relied upon and should be independently verified with primary sources of information. Taylor and Francis shall not be liable for any losses, actions, claims, proceedings, demands, costs, expenses, damages, and other liabilities whatsoever or howsoever caused arising directly or indirectly in connection with, in relation to or arising out of the use of the Content.

This article may be used for research, teaching, and private study purposes. Any substantial or systematic reproduction, redistribution, reselling, loan, sub-licensing, systematic supply, or distribution in any form to anyone is expressly forbidden. Terms &

Mol. Cryst. Liq. Cryst., Vol. 580: pp. 39–46, 2013
Copyright © Taylor & Francis Group, LLC
ISSN: 1542-1406 print/1563-5287 online
DOI: 10.1080/15421406.2013.803912

Surface Engineering of Zinc Oxide Nanoparticles by Biocompatible PPEGMA Polymer: Synthesis, Characterization, and Optical Property Studies

MD. RAFIQUL ISLAM,[1] LONG GIANG BACH,[1] SANG-JIN JUNG,[2] YEONG-SOON GAL,[3] AND KWON TAEK LIM[1,*]

[1]Department of Imaging System Engineering, Pukyong National University, Busan, Korea
[2]Department of Advanced Materials Engineering, Kyungsung University, Busan, Korea
[3]College of General Education, Kyungil University, Kyungsangbuk-Do, Hayang, Korea

The poly[poly(ethylene glycol) monomethacrylate] (PPEGMA) grafted ZnO nanoparticles (NPs) were successfully prepared using in situ free radical polymerization strategy. Initially, surface of ZnO NPs was modified by 3-(trimethoxysilyl)propyl methacrylate (TMSPMA), subsequently AIBN initiated copolymerization of PEGMA from ZnO NPs afforded well defined PPEGMA-g-ZnO nanocomposites. FT-IR and XPS confirmed the chemical grafting of polymer onto ZnO NPs. The XRD data suggested the zincite structure in the nanocomposites. The immobilization of polymer onto NPs was observed in SEM images. Thermal property was analyzed by TGA. The UV-vis and photoluminescence (PL) studies of the nanocomposites suggested an enhanced optical properties.

Keywords Free radical polymerization; optical properties; surface modification; ZnO nanoparticles

1. Introduction

Nanoparticles have been the subject of recent scientific and technological interest due to their fascinating size dependent physicochemical and optoelectronic properties. The inorganic–polymer hybrid nanomaterials demonstrate the properties of both the inorganic nanoparticles and the polymer by combining thermal stability, mechanical strength, electronical and optical properties of inorganics with flexibility and the processing ability of polymer. Consequently, these nanocomposites offer promising applications in diverse areas such as photocatalysis, lithography, optics, biotechnology and electronic devices [1,2]. Many efforts have been concentrated on the design and fabrication of polymer/inorganic nanocomposites. A number of different metal and metal oxide nanoparticles (NPs) have so far been encapsulated by the shell of polymers, giving rise to a host of nanocomposites [3,4].

---

[*] Address correspondence to Kwon Taek Lim, Department of Imaging System Engineering, Pukyong National University, 599-1 Daeyeon 3-Dong, Nam-Gu, Busan 608-737, Korea (ROK). Tel.: (+82)-51-629-6409; Fax: (+82)-51-629-6408. E-mail: ktlim@pknu.ac.kr

Generally, there are two main ways to modify the surface of NPs: physical and chemical methods. Chemical surface modification is the most promising strategy because of the strong covalent bond formation between the surface modified particles and polymer chains. Moreover, introduction of double bonds onto the surface of NPs can be copolymerized with other vinyl monomers so that dispersibility of NPs would be improved [5,6]. The incorporation of the initiating groups onto the surface of the NPs usually need multi-step reaction, while the introduction of the double bonds can be achieved by one-step synthesis using silane coupling agent containing double bonds to modify the surface of the NPs.

Considering the simplicity, *in situ* free radical polymerization of vinyl monomers with surface bound double bond shows a great promise. ZnO NPs is a semiconductor material with huge potential applications such as gas sensors, piezoelectric transducers, optical waveguides, UV-laser emitters and solar cells, antibacterial reagent, conductive glass etc. [7–10]. Among many other polymers, the poly(ethylene glycol) monomethacrylate (PEGMA) is known to be biocompatible, nonimmunogenic, nonantigenic and miscibility with many solvents and are finding an ever-expanding range of biomedical and industrial applications. Moreover, the end hydroxyl groups of the grafted PEGMA polymer (PPEGMA)) side chains can be post-modified into various functional derivatives [11,12]. Well incorporation of ZnO NPs in PPEGMA matrix was expected to achieve nanocomposites of unique properties. In this work, a simple protocol for the covalent immobilization of PEGMA polymer onto ZnO NPs employing *in situ* polymerization has been discussed.

2. Experimental Details

2.1. Materials

PEGMA ($M_n = 300$) was passed through a silica gel column and stored under an argon atmosphere at 0°C. 2,2′-Azobisisobutyronitrile (AIBN) was purified by recrystallization from methanol. ZnO NPs (<100 nm) and 3-(trimethoxysilyl)propyl methacrylate (TMSPMA) were used as received.

2.2. Functionalization of ZnO NPs by TMSPMA

In 500 mL three-neck round bottom flask, 20 g of TMSPMA was added to the dispersion of 10 g of ZnO NPs in 200 mL of toluene. The resulting mixture was stirred at room temperature under a stream of argon for 20 h. After reaction, TMSPMA-*f*-ZnO NPs were separated by centrifugation and washed repeatedly with toluene. Finally, the powder was dried at 30°C for 24 h under vacuum.

2.3. Synthesis of PPEGMA-g-ZnO Nanocomposites Via in situ Free Radical Polymerization

The PPEGMA-*g*-ZnO nanocomposites were synthesized through *in situ* free radical polymerization by one step method. TMSPMA-*f*-ZnO NPs (1 g), PEGMA (5 mL), AIBN (0.05 g) and deionized water (10 mL) were taken in a 100 mL round bottom flask. The mixture was kept in ultrasonic vibrations for 30 min and then, the mixture was stirred under nitrogen at 65°C for 12 h. After polymerization, the flask was cooled to room temperature and the reaction mixture was precipitated in methanol. The product was filtered and dried in a vacuum oven for 24 h.

2.4. Instrumentation

FT-IR analysis of the samples was performed using a BOMEM Hartman & Braun FT-IR spectrometer. Surface composition of the samples was studied by X-ray Photoelectron Spectroscopy (XPS, Thermo VG Multilab 2000). Scanning electron microscopy (SEM) images of samples were captured with Hitachi JEOL- JSM-6700F system. Thermogravimetric analysis (TGA) was conducted with Perkin-Elmer Pyris 1 analyzer. The crystallographic state of the nanocomposites was studied by a Philips X'pert-MPD system diffractometer. The optical properties of the products were measured by ultraviolet spectroscopy (Perkin-Elmer Lambda 40) and photoluminescence spectroscopy (Hitachi F-4500) at room temperature.

3. Results and Discussion

ZnO NPs were covalently grafted by PPEGMA via *in situ* free radical polymerization (Scheme 1). Prior to polymerization, ZnO NPs were treated with the TMSPMA, a silane coupling agent having C=C bond, to introduce organic functional moieties on the surface of ZnO NPs *via* ligand-exchange between the hydroxyl groups on the surface of ZnO NPs and trimethoxyliane groups of TMSPMA. Therefore, dangling double bonds to some extent remain on the surface of functionalized ZnO NPs, allowing them to further graft into PPEGMA matrices.

Scheme 1. Schematic illustration for the preparation of PPEGMA-*g*-ZnO nanocomposites.

FT-IR spectra of ZnO NPs, TMSPMA-*f*-ZnO NPs and PPEGMA-*g*-ZnO nanocomposites are shown in Fig. 1. In the FT-IR spectrum of ZnO NPs (Fig. 1A), the band at 492 cm^{-1} is the characteristic absorption of Zn—O bond and the broad absorption band at 3427 cm^{-1} is attributed to the absorption of hydroxyl groups. In the spectrum of TMSPMA-*f*-ZnO NPs (Fig. 1B), a broad absorption band in the range from 965 to 1140 cm^{-1} is assigned to the Si—O stretching. The absorptions at 2958, 1716 and 1636 cm^{-1} correspond to the stretching vibration of CH_3, C—O and C=C groups of TMSPMA, respectively. A broad band at 1101 cm^{-1} is ascribed to the C—O—C group, the relatively increase absorption bands at 2850 and 2922 cm^{-1} attributed to CH_2 stretching vibrations and the band at 1723 cm^{-1} is ascribed to the C=O stretch of PEGMA are clearly observed in the spectrum of PPEGMA-*g*-ZnO nanocomposites (Fig. 1C). These FT-IR results strongly suggest that the PPEGMA chains were attached to the surfaces of ZnO NPs through covalent linkage.

XPS was employed to investigate surface chemical composition of the ZnO NPs, TMSPMA-*f*-ZnO NPs and PPEGMA-*g*-ZnO nanocomposites as shown in Fig. 2. In the spectrum of ZnO NPs, the characteristic photoelectron lines are observed at binding energy (BE) of about 10, 89, 139, 285, 531, 1021 and 1045 eV which are attributed to Zn3d, Zn3p, Zn3s, C1s, O1s, Zn2$p_{3/2}$ and Zn2$p_{1/2}$, respectively. TMSPMA tethering onto the ZnO NPs is evidenced with the appearance of Si signal at BE of 102 eV. The intensity of C1s in the XPS scan of PPEGMA-*g*-ZnO nanocomposites is higher than that of TMSPMA-functionalized

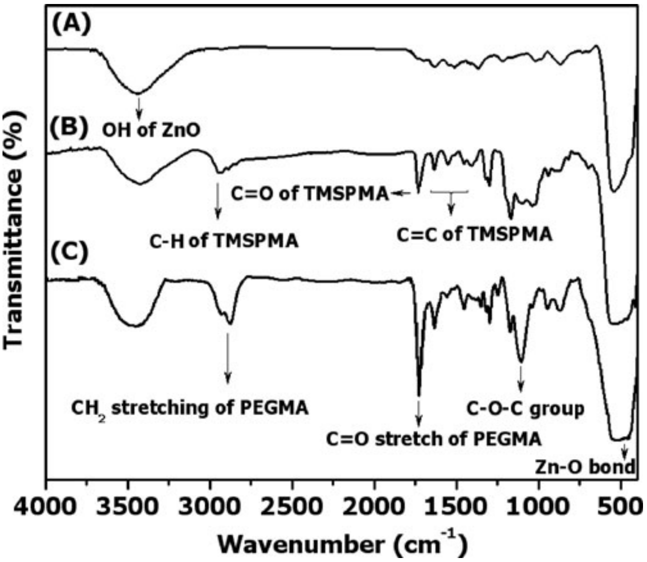

Figure 1. FT-IR spectra of (A) ZnO NPs, (B) TMSPMA-*f*-ZnO NPs, and (C) PPEGMA-*g*-ZnO nanocomposites.

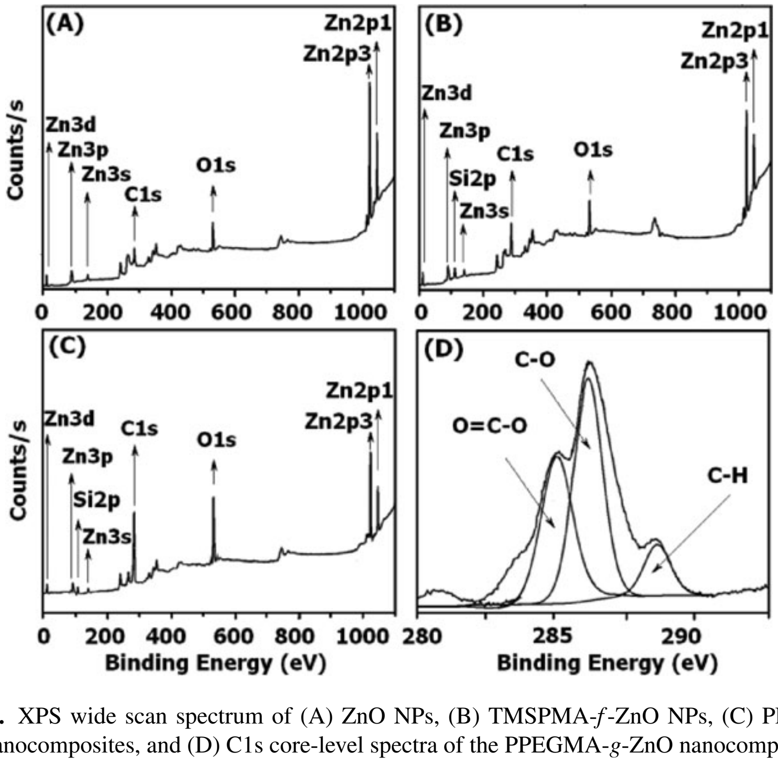

Figure 2. XPS wide scan spectrum of (A) ZnO NPs, (B) TMSPMA-*f*-ZnO NPs, (C) PPEGMA-*g*-ZnO nanocomposites, and (D) C1s core-level spectra of the PPEGMA-*g*-ZnO nanocomposites.

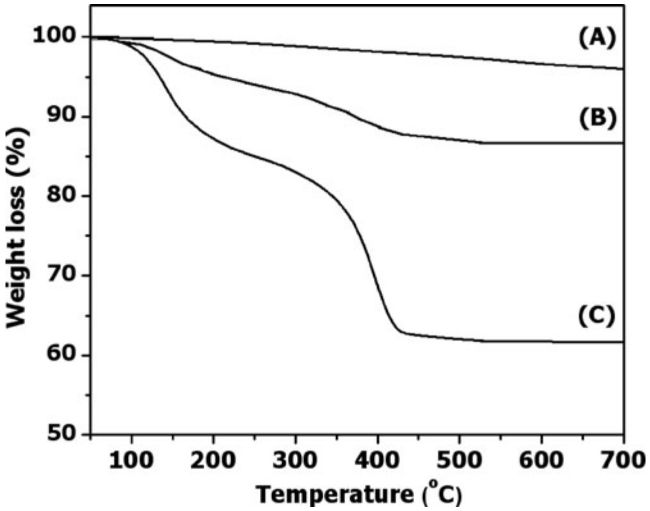

Figure 3. TGA curves of (A) ZnO NPs, (B) TMSPMA-*f*-ZnO NPs and (C) PPEGMA-*g*-ZnO nanocomposites.

ZnO NPs (Fig. 2C), indicating that the polymeric chains were grafted on the surfaces of NPs. The C1s core-level spectrum of PPEGMA-*g*-ZnO nanocomposites is curve-fitted with three peak components having BE at about 285, 286 and 288 eV, which are attributable to the O=C—O, C—O, and C—H species, respectively.

To study the thermal behavior and degree of grafting of PPEGMA onto ZNO NPs, TGA studies of the samples were undertaken (Fig. 3). The pristine ZnO NPs show a weight loss of *ca.* 4.1% while heating from 50 to 700°C, due to the elimination of physically and chemically adsorbed water, and the decomposition of hydroxide groups available on the surface of ZnO NPs (Fig. 3A). The TMSPMA-*f*-ZnO NPs exhibit weight loss of *ca.* 13.2%. In compare with pristine ZnO NPs and TMSPMA-*f*-ZnO NPs, the total weight loss of PPEGMA-*g*-ZnO nanocomposites was much higher due to the presence of significant amount of PPEGMA polymer (Fig. 3C). The degree of grafting of PPEGM onto ZnO NPs was calculated to be 25.6%.

To investigate the influence of covalent incorporation of ZnO NPs in the polymer matrix, the modified ZnO NPs were studied by FE-SEM. In the micrograph, the crystallite of ZnO NPs can easily be recognized (Fig. 4A). After polymerization, grafting of PPEGMA onto ZnO NPs can be observed by taking a close look at the FE-SEM image as shown in Fig. 4B. The shape of crystal of ZnO NPs was changed due to immobilization of soft polymer layer.

XRD analysis was performed to investigate the physical structure of modified ZnO NPs as shown Fig. 5. In the XRD patterns of the pristine ZnO NPs, the characteristic peaks at $2\theta = 31.92, 34.58, 36.41, 47.68, 56.74, 62.98, 66.50, 68.07$ and 69.21 which correspond to the (100), (002), (101), (102), (110), (103), (200), (112) and (201) reflections, respectively, are observed. The data are full agreement with the zincite structure of ZnO (JCPDS 5-0664). It is observed that the XRD patterns of TMSPMA-*f*-ZnO NPs and PPEGMA-*g*-ZnO nanocomposites are almost identical to that of the pristine ZnO NPs. In the nanocomposites, in addition to the analogous peaks, a broad peak at $2\theta = 19.8$ originated from polymer phase,

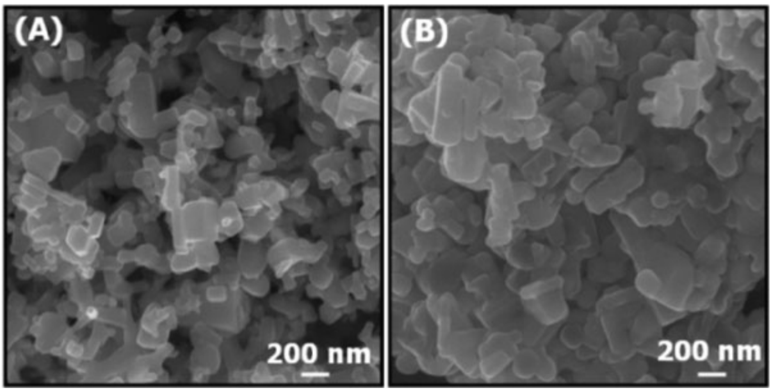

Figure 4. FE-SEM images of (A) ZnO NPs, and (B) PPEGMA-*g*-ZnO nanocomposites.

implying that the encapsulation of ZnO NPs by PPEGMA did not alter the crystallinity of the ZnO NPs.

It is known that the optical property of nanocomposites not only depend on the nature of the two segments, but also dependent on the preparation process of the materials. The surface state, dispersity, crystallinity and purity of ZnO NPs could be manipulated by varying preparation condition, as a result with the same compositions exhibit quite different optical properties. To investigate the optical properties of the modified ZnO NPs, the UV/vis absorption spectra of the samples were recorded as shown in Fig. 6. The absorption of the PPEGMA-*g*-ZnO nanocomposites extends the whole UV-vis region while the pristine ZnO NPs show absorption only in UV region (<400 nm). In the spectrum, it is observed that after covalent grafting, the absorption intensity was reduced along with a minor red shift. The absorption maxima of PPEGMA-*g*-ZnO nanocomposites displays at 382 nm

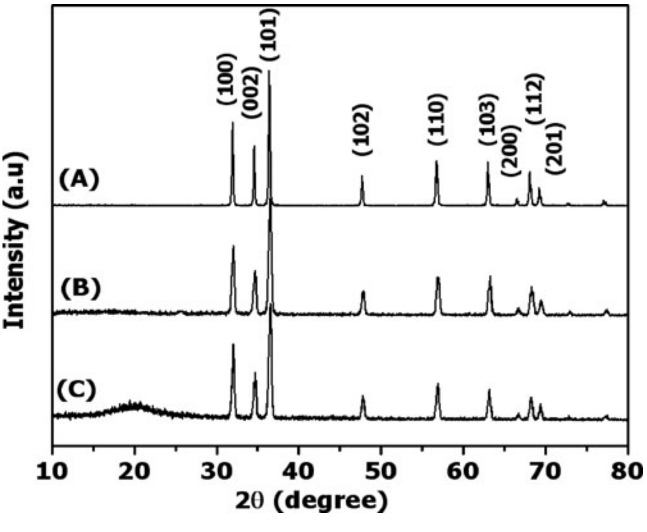

Figure 5. XRD patterns of (A) ZnO NPs, (B) TMSPMA-*f*-ZnO NPs, and (C) PPEGMA-*g*-ZnO nanocomposites.

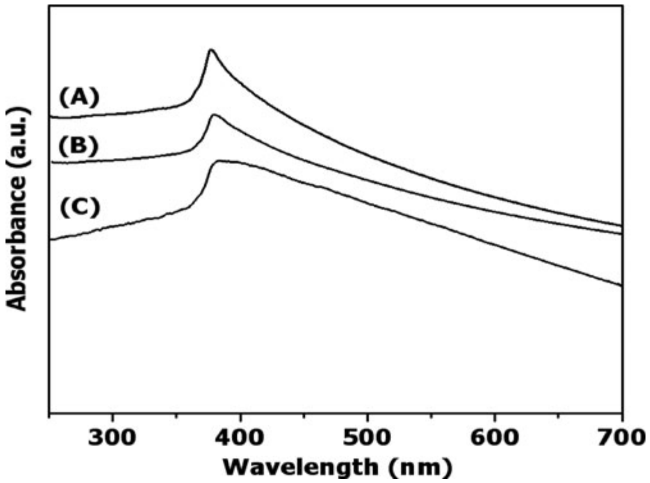

Figure 6. The UV-vis adsorption spectra of (A) ZnO NPs, (B) TMSPMA-*f*-ZnO NPs and (C) PPEGMA-*g*-ZnO nanocomposites.

corresponding to the exciton state in the bulk ZnO [8]. The grafting of PPEGMA onto ZnO NPs may introduce surface trap consequently resulted in red shift.

Figure 7 demonstrates the PL spectra of the ZnO NPs, TMSPMA-*f*-ZnO NPs and PPEGMA-*g*-ZnO nanocomposites with excitation at 325 nm. It is noticed that the nanocomposites displayed a strong ultraviolet band emission related to the free exciton emission and near-band-edge emission (NBE) corresponding to deep-level defects without any visible emissions. Moreover, the NBE emission of the PPEGMA-*g*-ZnO nanocomposites was enhanced as compared with the ZnO NPs. The phenomena can be explained in the way that

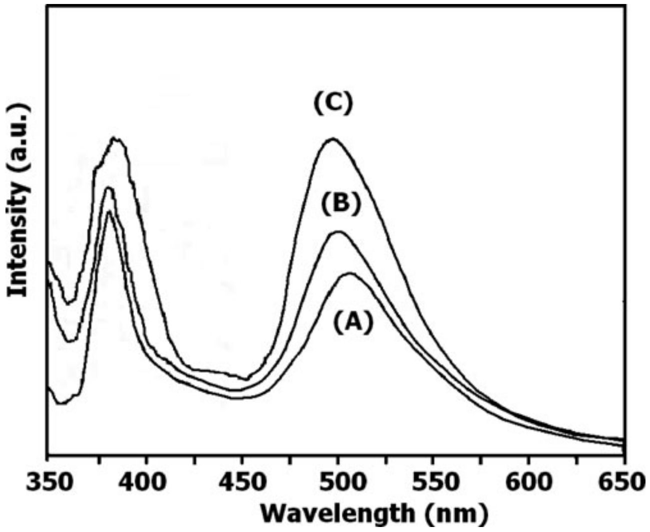

Figure 7. The PL spectra of (A) ZnO NPs, (B) TMSPMA-*f*-ZnO NPs, and (C) PPEGMA-*g*-ZnO nanocomposites.

covalent grafting of polymers onto ZnO NPs made the NPs well dispersed in the polymer matrices, so the ZnO luminescence was protected well and even enhanced because of easy exciton charge separation. The relative quantum yields (QYs) of ZnO NPs and PPEGMA-*g*-ZnO were measured using a solution of rhodamine 6G in ethanol (QY = 95%) as a reference material [13]. The QY of the PPEGMA-*g*-ZnO was found to be *ca*. 40.5% which was much higher than that of the ZnO NPs (23.6%).

4. Conclusions

The modification of ZnO NPs surface by silylating agent (TMSPMA) having double bond was revealed very effective to prepare PPEGMA-*g*-ZnO nanocomposites via *in situ* free radical polymerization strategy. The covalent bond formation between modified ZnO NPs and PPEGMA components was confirmed by FT-IR. The XPS results suggested the preparation of PPEGMA-*g*-ZnO nanocomposites. The grafting amount of PPEGMA was found to be *ca*. 25.6% as calculated by TGA. The SEM images of PPEGMA-*g*-ZnO nanocomposites depicted that ZnO NPs were encapsulated by PPEGMA polymer layers. XRD studies indicated the retention of zincite structure of ZnO NPs in the PPEGMA-*g*-ZnO nanocomposites. The UV-vis spectra of the PPEGMA-*g*-ZnO nanocomposites demonstrated a high optical transmittance in near UV-vis region. The PL studies suggested that PPEGMA-*g*-ZnO nanocomposites preserved the luminescence property of pristine ZnO NPs besides some extent enhanced emission intensity.

Acknowledgments

This work was financially supported by the Joint Program of Cooperation in Science and Technology through NRF grant funded by the MEST (No. 2011-0025680).

References

[1] Jeon, S., Yun, J., Lee, Y. S., Kim, & H. I. (2012). *J. Ind. Eng. Chem. 18*, 487.
[2] Bach, L. G., Islam, M. R., Jeong, Y. T., Gal, Y. S., & Lim, K. T. (2012). *Appl. Surf. Sci. 258*, 2816.
[3] Ray, S. S., & Okamoto, M. (2003). *Prog. Polym. Sci. 28*, 1539.
[4] Achilleos, D. S., & Vamvakaki, M. (2010). *Materials*., *3*, 1981.
[5] Guo, L., Chen, S., & Chen, L. (2007). *Colloid Polym. Sci*., *285*, 1593.
[6] Xu, D., Wang, M., Ge, X., Lam, M. H. W., & Ge, X. (2012). *J. Mater. Chem*., *22*, 5784.
[7] Ozgur, U., Alivov, Ya. I., Liu, C., Teke, A., Reshchikov, M. A., Dogan, S., Avrutin, V., Cho, S. J., & Morkoc, H. (2005). *J. Appl. Phys. 98*, 041301.
[8] Karunakaran, C., Rajeswari, V., & Gomathisankar, P. (2011). *Solid State Sci*., *13*, 923.
[9] Sato, M., Kawata, A., Morito, S., Sato, Y., & Yamaguchi, I. (2008). *Eur. Polym. J*., *44*, 3430.
[10] Charinpanitkul, T., Nartpochananon, P., Satitpitakun, T., Wilcox, J., Seto, T., & Otani, Y. (2012). *J. Ind. Eng. Chem. 18*, 469.
[11] Jeong, U., Teng, X., Wang, Y., Yang, H., & Xia, Y. (2006). *Adv. Mater*., *19*, 33.
[12] Wang, S., Zhou, Y., & Sun, W. (2009). *Mater. Sci. Eng. C 29*, 1196.
[13] Fischer M., & Georges, J. (1996). *Chem. Phys. Lett. 206*, 115.